Proceedings of the 46th International School and Conference on the Physics of Semiconductors "Jaszowiec" 2017, Szczyrk

Analysis of Optical Properties of MoS_2 Monolayer using Minimal-Basis Tight-Binding Models

N. Nouri[a,b,*], P. Potasz[b], S. Zia Borujeni[c], A. Wójs[b] and G. Rashedi[a]

[a]Department of Physics, Faculty of Sciences, University of Isfahan, Isfahan 81746-73441, Iran

[b]Department of Theoretical Physics, Wrocław University of Science and Technology, Wrocław, Poland

[c]Department of Mathematics, Faculty of Sciences, Tehran Central Branch, Islamic Azad University, Tehran, Iran

Optical properties of transition metal dichalcogenides monolayer of MoS_2 are analyzed using multi-orbital tight-binding models with only Mo d-orbitals (three-band model) and with an inclusion of S p-orbitals (six-band model). We look at band structures, momentum matrix elements between valence and conduction band, and joint optical density of states. Good agreement between the two models is shown in a vicinity of K point of the Brillouin zone. On line connecting K and Γ points, a local conduction band minimum at Q point is recovered only by six-band model in agreement with density functional theory and experimental results. We show that optical transitions at this point are active for both light polarizations. A peak in joint optical density of states is also seen at this point suggesting its potentially important role in a proper description of excitonic effects.

DOI: 10.12693/APhysPolA.132.313

PACS/topics: 73.20.At, 78.67.–n, 78.20.Bh

1. Introduction

Transition metal dichalcogenides (TMDs) monolayers are semiconductors that have attracted much attention due to their potential technological applications in electronic and optoelectronic devices [1–4]. They are characterized by the direct band gap at the corners of the hexagonal Brillouin zone, K and K' points, and valley-dependent optical selection rules related to the nearby band structure topology [5–8]. Experimental proofs of dynamical pumping of valley polarization by circularly polarized light in monolayers of TMDs was presented by several groups [9–12].

The optical properties of monolayer TMDCs are usually studied using effective models well describing vicinity of K and K' points, neglecting a proper description of complicated band dispersion at other areas of the Brillouin zone [13–15]. At first side this seems to be reasonable as optical properties are governed by excitations in a vicinity of the band gap [2–7, 15]. On the other hand, density functional theory (DFT) and experimental results show the second conduction band minimum on $K-\Gamma$ line at Q point [8] and at C point [16], respectively. This conduction band minimum is responsible for indirect $(K-Q)$ to direct $(K-K)$ band gap transition when a number of monolayers of TMDs is reduced to one. The importance of taking the Q point into account, and in general accurate description of the lowest conduction band in studies of optical properties of TMDs monolayers was not established yet.

In this work, we investigate optical properties of MoS_2 monolayer using three-band [13] and recently derived six-band tight-binding models [17]. A crucial difference between the two models is an inclusion, besides Mo d-orbitals are considered in three-band model, also S p-orbitals within six-band model. This allows for more accurate description of the lowest conduction band, leading to good fit to experimental and DFT results along $K-\Gamma$ direction of the Brillouin zone. We focus on band structures obtained within the models, momentum matrix elements between valence to conduction bands, and joint optical density of states. We show important relations between the models and emphasize the differences that lead to more accurate description of optical properties of MoS_2 in six-band model.

2. Models

MoS_2 monolayer consists of two sites within a unit cell corresponding to Mo atom (A site) and S dimer (B site), forming a honeycomb lattice. Three-band model derived in Ref. [13] is restricted to the description of Mo d-orbitals, that form a triangular lattice, neglecting completely S p-orbitals. Within the six-band model derived in Ref. [17], besides Mo d-orbitals, also S p-orbitals, $l=1$, with $m_p = 0, \pm 1$ are included. In order to properly fit band structures to DFT results, the three-band model introduces up to the third-nearest-neighbour hopping integrals while the six-band model only up to the next nearest neighbor hopping integrals. The band structure of the three-band model reproduced from Ref. [13] is shown in Fig. 1 on the left, and compared with the band structure of the six-band model reproduced from Ref. [17], on the right. In a vicinity of K valley, both models give similar results predicting direct band gap at this point. Within the six-band model, the second conduction band minimum at Q point, indicate by a star, is clearly seen. A proper description of a $K-\Gamma$ line in this model is the main difference in comparison to the three-band model. In the next section we analyze its importance when optical properties are studied.

*corresponding author; e-mail: nafise.nour@sci.ui.ac.ir

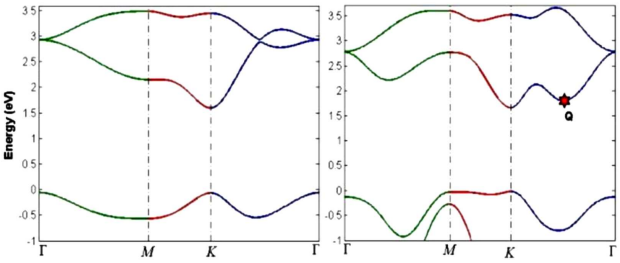

Fig. 1. Band structure of MoS_2 monolayer calculated using three-band model (left) and six-band model (right). Within six-band model a secondary conduction band minimum at Q point at an intermediate k value between K and Γ points is recovered, indicated by a star.

3. Results and discussion

We calculate the momentum matrix elements between single-particle states as they determine optical selection rules. Momentum matrix elements between the conduction and valence band eigenstates of the Hamiltonian are given by

$$P^{vc}(\boldsymbol{k}) = \frac{m_0}{\hbar}\langle v, \boldsymbol{k}|\nabla_k H|c, \boldsymbol{k}\rangle, \tag{3.1}$$

where m_0 is electron mass, and v and c refer to valence and conduction eigenstates, respectively [15]. For circular polarizations, we have

$$P^{vc}_{\pm}(\boldsymbol{k}) = \frac{1}{\sqrt{2}}\left[P^{vc}_x(\boldsymbol{k}) \pm \mathrm{i}P^{vc}_y(\boldsymbol{k})\right], \tag{3.2}$$

where $P^{vc}_x(\boldsymbol{k})$ and $P^{vc}_y(\boldsymbol{k})$ are x- and y-components of Eq. (3.1).

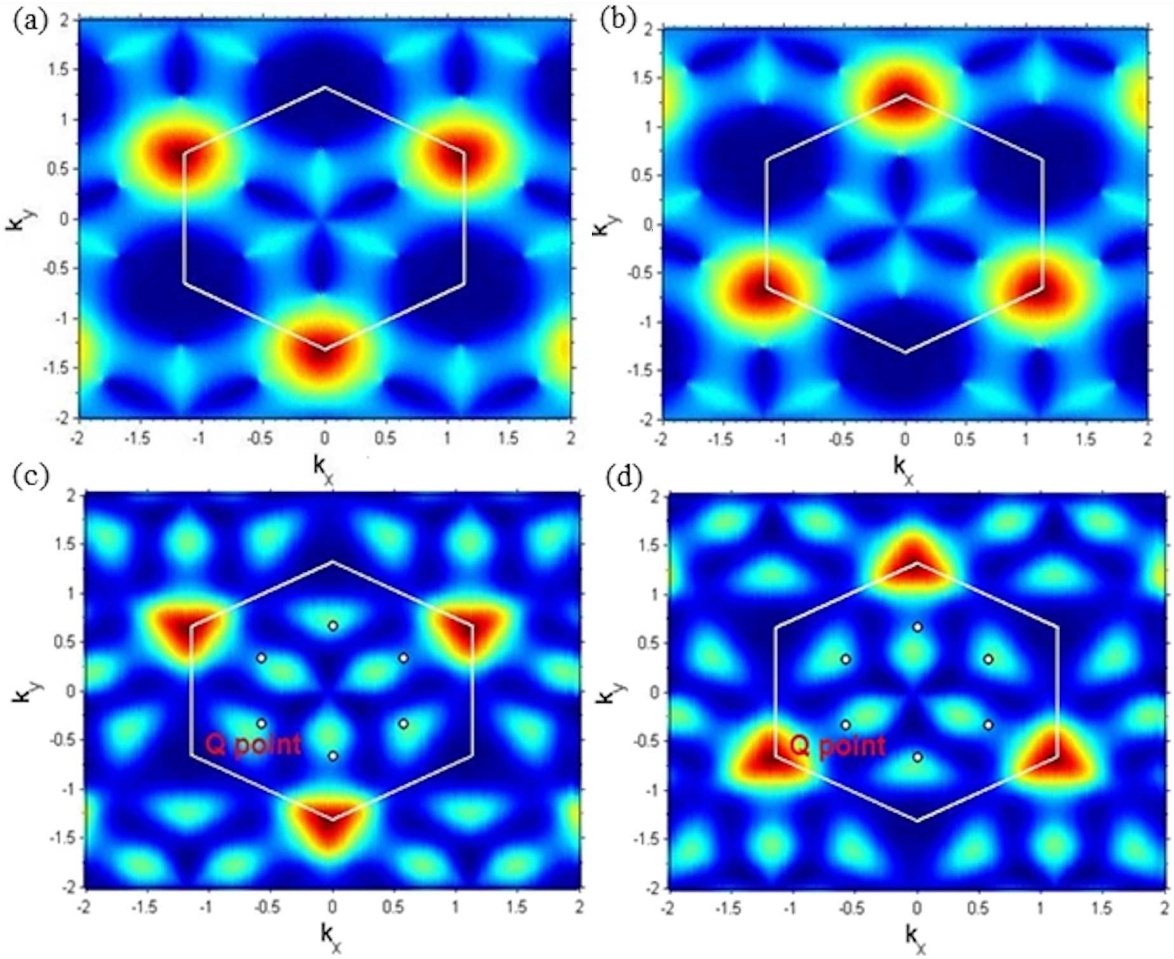

Fig. 2. Valence to lowest conduction band momentum matrix elements squared for two circular polarizations, for three-band model: (a) P_+ and (b) P_-, and six-band model (c) P_+ and (d) P_-. Red colour corresponds to maximal value and dark blue to zero. A white frame indicates boundary of the Brillouin zone.

In Fig. 2 we show momentum matrix elements squared for two circular polarizations P_+ and P_- for three-band (a) and (b), and six-band (c) and (d), models. Results are qualitatively similar in a vicinity of corners of the Brillouin zone, at K and K' points, where valley-dependent optical selection rules are recovered, see red areas around three K points and vanishing momentum matrix elements around K' points for P_+, and inversely for opposite polarization. Around these points threefold rotational symmetry is more clearly seen within six-band model. At the other areas of the Brillouin zone differences between the models are more evident. Especially, nonzero values of P_+ and P_- around Q points, indicated here by white circles, can be noticed only within six-band model.

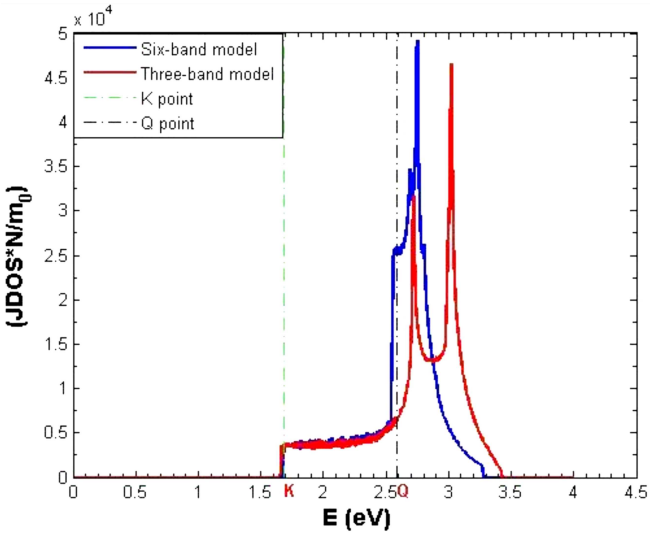

Fig. 3. Joint optical density of states as a function of transition energy calculated for whole Brillouin zone for MoS_2 monolayer using three-band model (red) and six-band model (blue). Green dash and black dash-dotted lines indicate K and Q points, respectively.

We summarize analysis of optical properties of MoS_2 by looking at joint optical density of states, shown in Fig. 3. Very good agreement between both models is seen for an energy range between the band gap at K point around $E = 1.6$ eV and up to $E = 2.5$ eV. Above $E = 2.5$ eV, a large signal coming from Q point of the Brillouin zone is noticed within six-band model, not seen within three-band model, confirming results presented in Fig. 2. Two singular peaks seen for three-band model comes from transitions at M point, at lower energy, and other points in the Brillouin zone. Within six-band model, they overlap, forming one broader singular peak around $E = 2.7$ eV.

4. Conclusions

We have analysed optical properties of MoS_2 monolayer using six-band and three-band tight-binding models. We look at momentum matrix elements between valence and conduction band and joint optical density of states. Both models give qualitatively similar results in a vicinity of the energy band gap, around K point of the Brillouin zone. Valley dependent polarization is observed. Some differences between the results for the two models are seen for larger energies resulting in distinguished joint optical density of states further from the energy gap, above 2.5 eV. Especially, optical transitions from Q-point gives large peak captured only by six-band model, active for both light polarizations.

Acknowledgments

The authors acknowledge partial financial support from National Science Center (NCN), Poland, grant Maestro No. 2014/14/A/ST3/00654.

References

[1] M. Chhowalla, H.S. Shin, G. Eda, L.J. Li, K.P. Loh, H. Zhang, Nature Chem. **5**, 263 (2013).

[2] Q.H. Wang, K. Kalantar-Zadeh, A. Kis, J.N. Coleman, M.S. Strano, Nat. Nanotechnol. **5**, 699 (2012).

[3] H.R. Gutiérrez, N. Perea-López, A.L. Elías, A. Berkdemir, B. Wang, R. Lv, F. López-Urías, V.H. Crespi, H. Terrones, M. Terrones, Nano Lett. **13**, 3447 (2012).

[4] A.M. Van Der Zande, P.Y. Huang, D.A. Chenet, T.C. Berkelbach, Y. You, G.H. Lee, T.F. Heinz, D.R. Reichman, D.A. Muller, J.C. Hong, Nat. Mater. **12**, 554 (2013).

[5] A. Splendiani, L. Sun, Y. Zhang, T. Li, J. Kim, C.-Y. Chim, G. Galli, F. Wang, Nano Lett..**10**, 1271 (2010).

[6] K.F. Mak, C. Lee, J. Hone, J. Shan, T.F. Heinz, Phys. Rev. Lett. **105**, 136805 (2010).

[7] D. Xiao, G.-B. Liu, W. Feng, X. Xu, W. Yao, Phys. Rev. Lett. **108**, 196802 (2012).

[8] E.S. Kadantsev, P. Hawrylak, Solid State Commun. **152**, 909 (2012).

[9] T. Cao, G. Wang, W. Han, H. Ye, C. Zhu, J. Shi, Q. Niu, P. Tan, E. Wang, B. Liu, J. Feng, Nat. Commun. **3**, 887 (2012).

[10] K.F. Mak, K. He, J. Shan, T.F. Heinz, Nat. Nanotechnol. **7**, 494 (2012).

[11] H. Zeng, J. Dai, W. Yao, D. Xiao, X. Cui, Nat. Nanotechnol. **7**, 490 (2012).

[12] S. Wu, J.S. Ross, G.-B. Liu, G. Aivazian, A. Jones, Z. Fei, W. Zhu, D. Xiao, W. Yao, D. Cobden, X. Xu, Nat. Phys. **9**, 149 (2013).

[13] G.B. Liu, W.Y. Shan, Y. Yao, W. Yao, D. Xiao, Phys. Rev. B **88**, 085433 (2013).

[14] A. Kormanyos, V. Zolyomi, N.D. Drummond, P. Rakyta, G. Burkard, V.I. Falko, Phys. Rev. B **88**, 045416 (2013).

[15] T.C. Berkelbach, M.S. Hybertsen, D.R. Reichman, Phys. Rev. B **88**, 085413 (2015).

[16] D. Kozawa, R. Kumar, A. Carvalho, K.K. Amara, W. Zhao, S. Wang, M. Toh, R.M. Ribeiro, A.H. Castro Neto, K. Matsuda, G. Eda, Nat. Commun. **5**, 4543 (2014).

[17] M. Bieniek, M. Korkusiński, L. Szulakowska, P. Potasz, I. Ozfidan, P. Hawrylak, arXiv:1705.02917.